Organic & Biomolecular Chemistry

Accepted Manuscript

This is an *Accepted Manuscript*, which has been through the Royal Society of Chemistry peer review process and has been accepted for publication.

Accepted Manuscripts are published online shortly after acceptance, before technical editing, formatting and proof reading. Using this free service, authors can make their results available to the community, in citable form, before we publish the edited article. We will replace this *Accepted Manuscript* with the edited and formatted *Advance Article* as soon as it is available.

You can find more information about *Accepted Manuscripts* in the Information for Authors.

Please note that technical editing may introduce minor changes to the text and/or graphics, which may alter content. The journal's standard Terms & Conditions and the Ethical guidelines still apply. In no event shall the Royal Society of Chemistry be held responsible for any errors or omissions in this *Accepted Manuscript* or any consequences arising from the use of any information it contains.

ROYAL SOCIETY OF CHEMISTRY

www.rsc.org/obc

Journal Name

RSCPublishing

ARTICLE

Rational design of a new fluorescent 'ON/OFF' xanthene dye for phosphate detection in live cells

Cite this: DOI: 10.1039/x0xx00000x

A. Martínez-Peragón,[a] D. Miguel,[a] A. Orte, [b] A. J. Mota, [c] M. J. Ruedas-Rama, [b] J. Justicia,[a] J. M. Álvarez-Pez,[b] J. M. Cuerva,[*a] and L. Crovetto[*b]

Received 00th January 2012,
Accepted 00th January 2012

DOI: 10.1039/x0xx00000x

www.rsc.org/

A new fluorescein derivative with ON/OFF features, 9-[1-(4-tert-butyl-2-methoxyphenyl)]-6-hydroxy-3H-xanthen-3-one (Granada Green, **GG**), was designed and synthesised. The new dye has spectral characteristics similar to those of other xanthenic derivatives but shows a higher pK_a value for the equilibrium between its neutral and anionic forms. In addition, **GG** undergoes the same phosphate-mediated excited state proton transfer (ESPT) reaction as other xanthenic derivatives, giving rise to fluorescence decay traces that are dependent on both the phosphate concentration and the pH of the medium. The phosphate-mediated ESPT reaction was employed to detect changes in the phosphate concentrations in live, permeabilised MC3T3-E1 preosteoblasts at pH 7.35. Its high pKa value indicates that this new dye is more sensitive as an intracellular phosphate sensor than other previously tested dyes, as experimentally demonstrated by its ability to detect a wider range of phosphate concentrations in biomimetic media and by the increased ratio of the phosphate concentration/decay time.

Introduction

Fluorescence lifetime imaging microscopy (FLIM) is an attractive fluorescence technique for quantitative real-time sensing of biologically important targets inside living cells.[1-3] In addition to the high sensitivity and non-invasive character of fluorescence methods, FLIM is an excellent alternative to fluorescence intensity and fluorescence ratiometric measurements because it is concentration independent and only a single excitation wavelength/emission interval is required.[4] The detection and quantification of phosphate inside live cells and in extracellular media is relevant in the study of bone mineralisation, signal transduction, and energy storage in biological systems.[5-7] Nevertheless, the development of fluorescence sensors for measuring phosphate under aqueous physiological conditions is challenging due to strong hydration effects.[8] Beyond invasive approaches employing radioactive phosphate, which are associated with a number of drawbacks,[9] there are few chemical sensors that are capable of detecting phosphate anions in an aqueous physiological system,[10] and none of them had successfully estimated the real-time concentration of phosphate inside live cells until the recently proposed xanthenic-based method.[11]

Fluorescein is a complex dye that, in aqueous solution at physiological pH, can exist in mono- and dianion prototropic forms. In two pioneering papers, we showed that at near-neutral pH and in the presence of 1 M phosphate buffer, which acts as a suitable proton donor-acceptor, the excited-state reaction that interconverts the mono- and dianion forms occurs very efficiently, and the fluorescence decays of these excited mono- and dianions become coupled; *i.e.*, the presence of these excited-state proton-transfer (ESPT) reactions influences the decay traces from excited fluorescein and causes the decay times to vary depending on both the pH and the phosphate concentration. On the contrary, at low phosphate concentrations (5 mM phosphate buffer or less), the excited monoanion and dianion are not coupled by the ESPT reaction and thus decay independently of each other.[12,13] The phosphate-mediated ESPT reaction is not exclusive to fluorescein, and the presence of phosphate also induces the ESPT reaction at near-neutral pH in other xanthenic derivatives, such as 2',7'-bis-(2-carboxyethyl)-5-(and-6)-carboxyfluorescein (BCECF).[14] However, the biexponential character of the fluorescence decays limits the use of those dyes as possible lifetime-based sensors because the close values of the two fluorescence decays prevent the use of the fluorescence lifetime imaging microscopy (FLIM) technique.[15] Moreover, although one of the coupled fluorescence decay times depends on the phosphate concentration in the medium, the other one is practically insensitive to phosphate.

Organic & Biomolecular Chemistry Accepted Manuscript

A few years ago, with the aim of developing new xanthenic dyes with improved spectral properties for specific purposes, it was proposed that the fluorescein structure could be divided into two parts: the benzoic acid moiety, as a photoinduced electron transfer (PeT) donor, and the xanthene ring as the fluorophore, in which PeT might determine the fluorescence quantum yield (ϕ_F). Thus, if the highest occupied molecular orbital (HOMO) energy level of the benzene moiety is higher than a certain threshold for electron transfer to the excited xanthene fluorophore (a-PeT), the ϕ_F is small.[16,17] In the opposite direction, electron transfer from the excited xanthene to the benzene moiety (d-PeT) can occur if the lowest unoccupied molecular orbital (LUMO) energy level of the benzene moiety is low enough, also resulting in small ϕ_F.[18] On the contrary, fluorescein derivatives with high ϕ_F should have benzene moieties with both low HOMO and high LUMO energy levels. Thus, the energy levels of the pendant aryl ring are directly related to the ϕ_F. It has also been shown that the role of the carboxylic group is only to keep the benzene ring and the xanthene moiety orthogonal to each other, and it can be replaced by any other substituents. Although there is some theoretical controversy about the direction of the PeT mechanism,[19] based on these ideas, new 9-aryl substituted fluoresceins were developed without the carboxylic acid in the pendant aromatic ring at C-9, which simplifies the number of prototropic species in aqueous solution. Thus, the so-called Tokyo Green dyes, 9-[1-(2-methyl-4-methoxyphenyl)]-6-hydroxy-3H-xanthen-3-one (2-Me-4-OMe TG) and 9-[1-(2-methoxy-5-methylphenyl)]-6-hydroxy-3H-xanthen-3-one (2-OMe-5-Me TG), do not have a carboxylic acid in the benzene ring, although this is kept orthogonal to the xanthenone core. Importantly, they have the advantage of being highly fluorescent at basic pH values (anion form of the xanthene moiety), but their quantum yield is near zero at acidic pH values (protonated form of the xanthene moiety).[20]

In our aim to find fluorescein derivatives capable of undergoing the characteristic phosphate-mediated ESPT reaction with a single lifetime in the near-neutral pH region, we study the photophysics of 2-Me-4-OMe TG and 2-OMe-5-Me TG in the presence of phosphate buffer in the pH range between 5 and 10.[21,22] The results showed that both undergo the characteristic ESPT reaction, in which the coupled fluorescence decay exhibits a phosphate-sensitive component on the order of nanoseconds and a second component on the order of subnanoseconds, whose value becomes negligible at pH and phosphate concentrations greater than 6.0 and 0.02 M, respectively. In addition, the larger decay time is highly sensitive to the phosphate concentration, while the presence of other ions not involved in the proton-transfer reaction has a negligible effect on the fluorescence decay time.[23] Therefore, the changes in the fluorescence decay time were considered a possible direct means of investigating the environmental phosphate concentration in a small volume at near neutral pH. Thus, in a recent paper, we used the ability of 2-Me-4-OMe TG to undergo phosphate-mediated ESPT to investigate the environmental phosphate concentration at physiological pH.[11] In this paper, it is shown that the dependence of the recovered long decay times from aqueous solutions of 2-Me-4-OMe TG on the phosphate concentration increases when the pH of the medium is near the pK_a of the dye. Because the pK_a of 2-Me-4-OMe TG and 2-OMe-5-Me TG and related derivatives are far from the physiological pH,[21,22] it is desirable to obtain fluorescent dyes with pK_a values that are higher and closer to the physiological pH than that of 2-Me-4-OMe TG.

In an attempt to increase the pK_a, one possible solution is to incorporate other aliphatic electron donating groups without modifying the optical properties of the dye. In this context, some alkyl groups have been added to the xanthene core, thus causing an increase in the pK_a values (fluorescein as a reference, pK_a 6.43; BCECF, pK_a 6.98; DHCF, pK_a 6.60; DEF, pK_a 6.61).[24-27] However, the synthetic procedures are not suitable for a great variety of substituents because of the harsh reaction conditions and the restriction thus imposed on the starting materials. Recently, 9-alkyl xanthenones with different aliphatic pendant groups have been easily prepared, and their photophysical behaviour has also been explored.[28] Remarkably, some of them retained similar fluorescent properties as those of fluorescein, including the characteristic phosphate-mediated ESPT reaction and higher pK_a values (6.20-6.67) compared with TGs (5.97-6.04).[21,22] Nevertheless, this approach to increase the pK_a without modifying the spectroscopic properties of the dye is limited by the electron donating nature of alkyl substituents. The best result has been achieved using an isopropyl group as a substituent (pK_a 6.67). Unfortunately, 9-alkyl xanthenones with better electron donating groups, such as the tert-butyl group, could not be prepared. Bearing all these precedents in mind, we thought that a tailor-made TG-type fluorescein might exhibit lower acidity, with a pK_a closer to the physiological pH. To this end, the substitution of the phenyl at C-9 is critical, and two synergic effects are required to destabilise the fluorescent anionic prototropic species: a) an electronegative oxygen atom must be placed near the xanthenone core to destabilise the anionic structure, and b) a good alkyl electron donating group must be used to increase the electron density in this oxygen without altering the desired molecular orbital ordering. After a theoretical screening, we prepared 9-[1-(4-tert-butyl-2-methoxyphenyl)]-6-hydroxy-3H-xanthen-3-one (Granada Green, **GG**), which is predicted to have a higher pK_a value than previously described TGs.

Experimental

Materials and solutions

For the photophysical studies, stock solutions of sodium phosphate were prepared using $NaH_2PO_4 \times H_2O$ and $Na_2HPO_4 \times 7H_2O$ (both Fluka, puriss. p.a.) in appropriate amounts to obtain the required pH. For the FLIM experiments, Dulbecco's modified Eagle's medium (DMEM, D-6546), α-minimum essential medium (α-MEM), foetal bovine serum (FBS), penicillin/streptomycin, trypsin-EDTA, and α-hemolysin from *Staphylococcus aureus* were obtained from Sigma Chemical (St. Louis, MO). To obtain the required phosphate concentration and pH in the measurement solutions, the necessary amount of phosphate stock solution was added to DMEM. The permeabilisation buffer contained 20 mM potassium MOPS pH 7.0, 250 mM mannitol, 1 mM potassium ATP, 3 mM $MgCl_2$, and 5 mM potassium glutathione. Commercially

Organic & Biomolecular Chemistry Accepted Manuscript

 This journal is © The Royal Society of Chemistry 2012

available phosphate-buffered saline (PBS) (Sigma-Aldrich) was also used to wash the cells. All solutions were prepared using Milli-Q water as the solvent. All chemicals were used as received without further purification. The solutions were kept cool in the dark when not in use to avoid possible deterioration by light and heat. Aliquots of α−toxin from *Staphylococcus aureus* were prepared and stored in a freezer (-20°C) until use.

Instrumentation

Absorption spectra were recorded on a Perkin-Elmer Lambda 650 UV/vis spectrophotometer with a temperature-controlled cell.

Steady-state fluorescence emission spectra were collected on a JASCO FP-6500 spectrofluorometer equipped with a 450 W Xenon lamp for excitation and with an ETC-273T temperature controller at 20 °C. The pH of the solutions was measured just before and after the fluorescence measurements at the same temperature.

Fluorescence decay traces of the compounds in the absence and in the presence of phosphate buffer were recorded by the single-photon timing method using a FluoTime 200 fluorometer (PicoQuant, Inc.). The excitation was performed by an LDH-485 (PicoQuant, Inc.), and the observation was made through a monochromator at different wavelengths. The pulse repetition rate was 20 MHz. Fluorescence decay histograms were collected in 1320 channels using 10 × 10 mm cuvettes. The time increment per channel was 36 ps. Histograms of the instrument response functions (using LUDOX scatterer) and sample decays were recorded until they typically reached 2×10^4 counts in the peak channel. The total width at half maximum of the instrument response function was ~ 60 ps. Fluorescence decays were recorded at three λ_{em} (505, 515 and 525 nm) for all samples. The fluorescence decay traces were individually analysed using an iterative deconvolution method with exponential models using FluoFit software (PicoQuant).

Cell culture.

MC3T3-E1 preosteoblast (ECACC 99072810) cell lines were provided by the Cell Culture Facility, University of Granada. MC3T3-E1 cells were grown in alpha minimum essential medium (αMEM) containing 10% foetal bovine serum and 1% penicillin–streptomycin in a humidified 5% CO_2 incubator, as described previously.[29] For the FLIM microscopy experiments, the cells were seeded onto 20-mm coverslips in 12-well plates at a density of 11,250 cells/cm^2. The coverslips were translated to the MicroTime 200 fluorescence lifetime microscope system (see below) and washed with PBS before adding the work solutions.

Cell permeabilisation.

MC3T3-E1 cells were deposited onto coverslips in 12-well plates and incubated with the described medium. On the day of the experiment, the cells were washed twice with phosphate-buffered saline (PBS) and were perforated by incubation for 15 min at 37°C with 2 μg/ml α-toxin in permeabilisation buffer.[30] Afterwards, the cells were washed twice with PBS and analysed by FLIM.

Ensemble Time-Resolved Fluorescence Instrumentation.

Fluorescence decay traces at the ensemble level were recorded using the time-correlated single photon timing (TCSPT)[31,32] method with a FluoTime 200 fluorometer (PicoQuant, Inc., Germany). The excitation source consisted of an LDH-485 pulsed laser with a minimum pulse width of 88 ps. The pulse repetition rate was 20 MHz. The laser pulse was directed to the solution sample in 10×10 mm cuvettes. The lens-focused fluorescence emission passed through a detection polariser set at the magic angle and a detection monochromator prior to reaching the photomultiplier detector. The fluorescence decay histograms were collected in 1,320 channels with a time increment of 36 ps/channel. Histograms of the instrument response functions (using LUDOX scatter) and sample decays were recorded until they reached approximately 2×10^4 counts in the peak channel.

FLIM instrumentation.

Fluorescence lifetime images were recorded with a MicroTime 200 fluorescence lifetime microscope system (PicoQuant GmbH) using the time-tagged time-resolved (TTTR) methodology, which permits fluorescence decay histograms to be reconstructed from molecules in the confocal volume for each pixel of the image. The excitation source consisted of the same LDH 485 nm pulsed laser described above, controlled by a "Sepia" driver (PicoQuant) and working at a repetition rate of 20 MHz. The excitation light beam crossed a quarter-wave plate and was directed into the specimen after being reflected in the excitation dichroic mirror (490dcxr, AHF/Chroma) to the oil immersion objective (1.4 NA, 100×) of an inverted confocal microscope (IX-71, Olympus). The collected fluorescence light was filtered by a long-pass filter HP500LP (AHF/Chroma) and focused onto a 75-μm pinhole. After the aperture, the fluorescence light crossed through an FF01-520/35 bandpass filter (Semrock) and was refocused onto an SPCM-AQR 14 single photon avalanche diode (Perkin Elmer). The data acquisition was performed with a TimeHarp 200 TCSPT module (PicoQuant GmbH) in TTTR mode, which enabled the reconstruction of the FLIM image. Raw images were recorded by raster scanning an area of 80×80 μm with a resolution of 512×512 pixels. The photons of each pixel were temporally sorted with respect to the excitation pulse in the histograms with a time resolution of 116 ps/channel.

Fluorescence decay traces and FLIM image analysis.

The fluorescence decay traces at the ensemble level were individually analysed using an iterative deconvolution method with exponential models using FluoFit software (PicoQuant). The FLIM images were analysed using the SymphoTime software (PicoQuant). To obtain the FLIM images, an instrument response function (IRF) was reconstructed from a monoexponential fluorescence decay trace of **GG** in solution. This was employed to analyse the fluorescence decay histogram in each pixel over the whole image by iterative

Organic & Biomolecular Chemistry Accepted Manuscript

deconvolution applying the maximum likelihood estimator (MLE), which yields correct parameter sets for low count rates.[33] Binning of 5×5 pixels and prehistogramming of 2 temporal channels (for a final resolution of 232 ps/channel) were used to achieve a larger number of counts in each pixel. For the analyses of **GG** in biomimetic media in the presence of different phosphate concentrations, a monoexponential decay model was set to fit the decay traces. For the experiments in the intracellular cytoplasm, a biexponential model was employed with a fixed decay time of 1.5 ns to account for the short-lived autofluorescence of the cell, whereas the second decay time was a freely adjustable parameter. To obtain the average value of the **GG** lifetime in the intracellular cytoplasm, the pixels in the region of interest (cellular cytoplasm) were selected, and a total fluorescence decay histogram of the region of interest was reconstructed and fit to a biexponential function using a fixed short decay time of 1.5 ns (lifetime arising from the interaction between the dye and the intracellular components and cell autofluorescence) and a freely adjustable long decay time (lifetime sensitive to phosphate concentration). The value of the long decay time is reported in figures 4 to 6.

Results and Discussion

We initially carried out theoretical calculations to find a suitable candidate to increase the pKa values of TGs without altering their photophysical properties. Within this context, we focused our attention on a family of xanthenones, **1-6** and **2-Me-4-OMe TG**. Several of these, xanthenones **1-5**, present an oxygenated function in the C-2´ of the aromatic ring located at C-9. We assumed that an increase in the electronic density in this oxygen atom would destabilise the anion formation. Theoretical calculations using Density Functional Theory (DFT) showed a good correlation between the donor capabilities of the alkyl group R[34] with the charge at the oxygen (Figure 1).

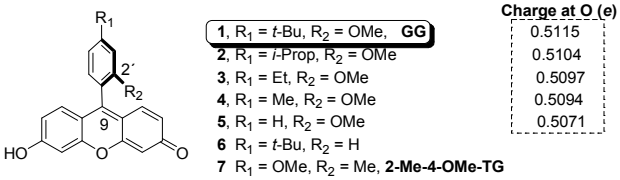

Figure 1. Evaluated structures and calculated charge.

Although the theoretical estimation of pK_a values is not a simple task,[35] the proton-transfer energy can be used qualitatively to compare structures.[36] In this case, we calculated the proton-transfer energy of selected structures **1** (**GG**), **5**, **6**, and **7** (**2-Me-4-OMe TG**). Using the proton-transfer reaction of **2-Me-4-OMe TG** as a reference, we observed the highest destabilising effect in compound **1** (Figure 2).[37] Moreover, the results for compounds **5** and **6** suggested that the value of ΔG was not only the sum of the effects of the oxygen atom at C-2´ (**5**) and the alkyl groups at C-4´ (**6**). In fact, a direct destabilising effect of the alkyl-donating group R on the xanthenone core could be ruled out because the benzene and xanthenone moiety are practically perpendicular.[38] Taking into account that an increase of one pK_a unit corresponds to 5.7 kJ mol^{-1} in free energy terms, a substantial increase in the pK_a value of **GG** is therefore expected.

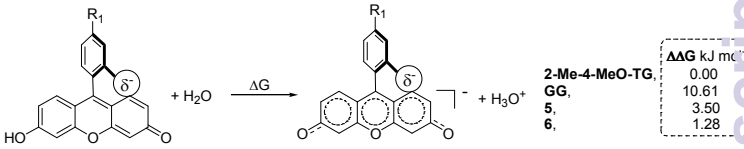

Figure 2. Proton-transfer energies of compounds **1 (GG)**, **5**, **6**, **7 (2-Me-4OMe-TG)**.

Additionally, it is critical that the new substitution not interfere with the photophysical properties of the dye. In this sense, Nagano proposed in 2004 that to preserve the fluorescence of the anion, the HOMO and LUMO levels of the xanthenone core must be placed between the HOMO and LUMO levels of the aryl substituent at C-9.[39] Theoretical calculations showed that in compound **1**, this prerequisite was attained (Figure 3). Bearing these precedents in mind, **GG** was selected as our synthetic objective.

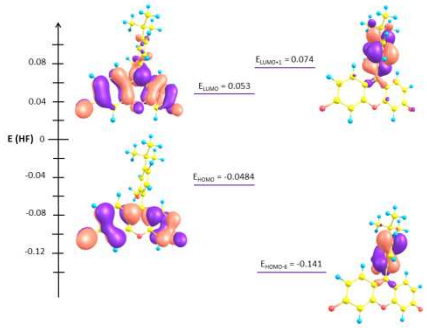

Figure 3. Schematic orbital diagram and isosurface plots of LUMO+1, LUMO, HOMO and HOMO-6.

Thus, **GG** was prepared in excellent yield (96 %) using a nucleophilic addition of the corresponding Grignard derivative of aryl bromide (**9**) to the TBDMS-protected 3,6-dihydroxy-xanthenone (**10**)[20] and subsequent dehydration with aqueous hydrochloric acid (Scheme 1). In this case, the *tert*-butyl group present in the final product fulfilled a dual role. This group was required to increase the pK_a value and was also required for the regioselective placement of the halogen in the bromide precursor **8**.

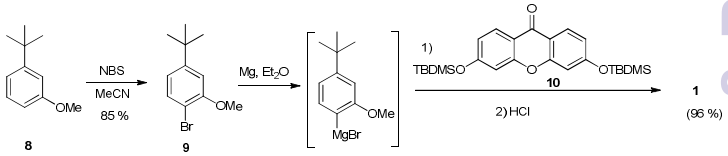

Scheme 1. Synthetic sequence for the preparation of compound **1**

Organic & Biomolecular Chemistry Accepted Manuscript

This journal is © The Royal Society of Chemistry 2012

Photophysics

The photophysical behaviour of **GG** in aqueous solutions at near-physiological pH has been studied by absorption and by steady-state and time-resolved emission spectroscopy.

The visible absorption spectra of aqueous solutions of **GG** in the pH range between 6 and 9 were recorded. The absorption spectral changes occurring in this pH region are dictated by the ground-state pK_a values. Since the isosbestic point was consistently around 455 nm at any phosphate concentration, we concluded that phosphate buffer does not significantly perturb the absorption spectrum of the aqueous **GG** solutions, and therefore, this compound does not form ground-state complexes with phosphate buffer. Figure 4 shows two prototropic forms and only one isosbestic point. Thus, a single ground-state pK_a is present in this pH range. The similarity of the spectral profiles of the two prototropic forms with those of the Tokyo Green family[21] suggests that the two visible absorbing forms correspond to the neutral and the anionic form.

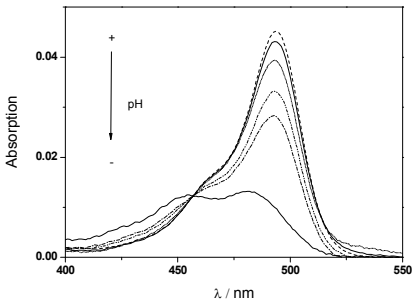

Figure 4. Absorption spectra of **GG** (at 7×10^{-6} M) in phosphate buffer (0.005 M) at pH values between 6 and 8. The arrow indicates decreasing pH values. The isosbestic point at 456 nm is clearly observed. For clarity, the Figure 4 only contains spectra from six solutions.

To recover the pK_a^{app} and the molar absorption coefficients ε_i (λ_{abs}) of the two acid-base species, a global fit of the absorbance *vs.* pH and *vs.* λ_{abs}[12] to the corresponding acid-base equilibrium equations was carried out (Figure S1). We obtained a pK_a^{app} value of 7.39 ± 0.07. The anionic form showed a peak at 495 nm with a value of $\varepsilon_{Anion}(495)$ =60480 ± 880.

At a constant excitation intensity, low absorbance values, and negligible rates of proton transfer in the excited state,[40-41] it is possible to determine the ground state acid-base equilibrium constant by fluorimetric titration. Therefore, steady-state fluorescence spectra were collected at an excitation wavelength of 490 nm from solutions in a pH range between 6 and 9.. Figure 5 shows the variations in fluorescence intensity with pH. These changes were in good agreement with the changes observed in the absorption spectra. A pK_a value of 7.26 ± 0.019 was obtained from the fit of the fluorescence experimental results. (Figue S2)

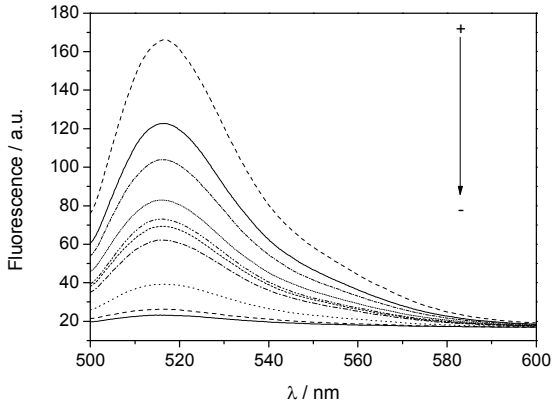

Figure 5. Steady-state emission spectra (λ_{ex} = 490 nm), of 7×10^{-6} M **GG** aqueous solutions at pH values between 6 and 9.

Quantum yield values from steady-state fluorescence measurements were calculated for the anion forms using fluorescein in 0.1 M NaOH as a reference (ϕ_{fluo} = 0.95). The quantum yield of the neutral form was obtained by fitting the steady-state fluorescence spectra to the equilibrium equation (see SI for details) once the values of ϕ_A were known. The recovered quantum yields were 0.97 and 0.10 for the anion and the neutral form, respectively.

The fluorescence decay traces in the absence of phosphate buffer were recorded in the pH range between 6 and 9 at one λ_{ex} = 485 nm and three λ_{em} (505, 515, and 525 nm). At all pH values, the decays followed a monoexponential decay function with a lifetime value of 3.97 ns, which was independent of pH. This result can be explained by the small contribution of the neutral form to fluorescence due to the low extinction coefficient at the excitation wavelength (485 nm) and its low fluorescence quantum yield.

Once the major spectral characteristics of **GG** near the physiological pH were recovered, we focused on the ESPT reaction between the dye and phosphate. We studied the absorption and emission spectra as a function of the phosphate buffer concentration at pH 7.35. We found that an increase in the phosphate buffer concentration in the range of 5 mM to 600 mM showed pronounced effects on the emission spectra but only weak effects (ionic strength) on the absorption spectra. The pronounced effects on the emission spectrum must therefore be due to the presence of the well-known ESPT reaction.[13] Thus, we studied the effect of the phosphate concentration by means of time-resolved fluorescence. The fluorescence decay traces should be influenced by the presence of ESPT reactions, causing the decay times to be dependent on the pH and on the phosphate concentration.[13,22] We recorded fluorescence decay traces from aqueous solutions of **GG** at pH 7.35 and at different phosphate buffer concentrations, C^B, ranging between 5 mM and 600 mM, as a function of λ_{ex} (485 nm) and λ_{em} (505, 515, and 525 nm). Figure 6 shows the recovered decay times at pH = 7.35 *vs.* phosphate concentration. The standard errors are obtained from the diagonal elements of the covariance matrix available from the global analysis fit of decay traces recorded at the three different emission wavelengths. and are between 0.020 and 0.032 ns**.** The decays were well analyzed by monoexponential functions, given

Organic & Biomolecular Chemistry Accepted Manuscript

good fitting parameters ($\chi_g^2 < 1.06$).From this plot, we observed that the change in the decay times was 0.1 ns higher than that previously obtained with 2-Me-4-OMe TG in the same phosphate buffer concentration range.[21]

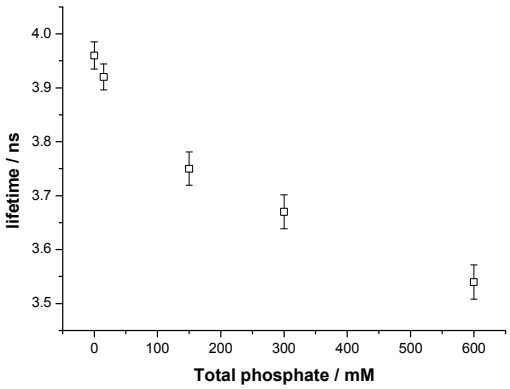

Figure 6. Recovered decay times at pH = 7.35 vs. [Phosphate].

Biomimetic media

FLIM technology is particularly attractive for intracellular sensing because of the advantages of time-resolved fluorescence techniques. Sensors based on emission intensity have several disadvantages for quantitative measurement because they are prone to concentration dependence, interference from cell autofluorescence, and several sources of optical excitation power drift. In contrast to intensity measurements, decay times are independent of the local concentration of the probe and are inherently robust in the presence of absorption and scattering, although they are still highly sensitive to changes in the environment.

If **GG** is intended to be employed as an intra-cellular sensor, the highly crowded intracellular environment could alter its response. Therefore, we tested the capability of the dye to estimate the concentration of phosphate in solutions mimicking the cytoplasm. Thus, **GG** was dissolved in solutions of Dulbecco's Modified Eagle's Medium at pH 7.35 in the presence of different phosphate concentrations in the 10 to 400 mM range. The dye was at a concentration of 1×10^{-7} M. The solutions were deposited on the surface of a microscope glass slide, and FLIM confocal images were recorded following the procedure described in the Experimental section. In Figure 7A, exemplary FLIM images from the samples are shown after applying an arbitrary colour scale to the recovered fluorescence decay times. The recovered images illustrate that the phosphate-response of the dye was maintained even in these crowded solutions. Considering the complexity of the matrix, the results are very acceptable, as the differences in the phosphate concentrations in the media were clearly observable. The average values of the fluorophore decay times (Figure 7B) were in good agreement with those obtained by conventional time-resolved fluorimetry in aqueous solutions (shown in Figure 6). The standard error calculated for the decay time of **GG** on the glass surface was consistently low, even though the decay time distributions were calculated from several FLIM images, which indicates the robustness of the technique. The overall frequency histograms of the decay times obtained from individual pixels of several images (at least three) collected under the same conditions clearly showed a shift in the decay time of the dye, allowing the phosphate response of the dye to be determined (Figure 7C).

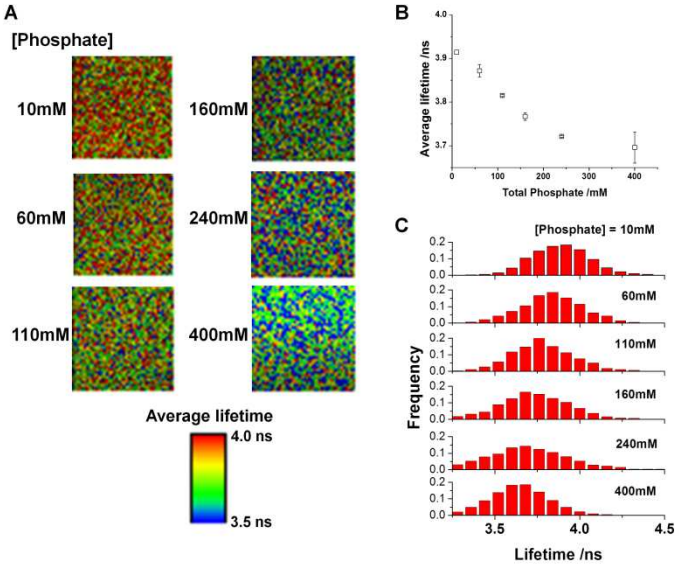

Figure 7. FLIM images (A), average decay time (B), and frequency lifetime histograms (C) of 1×10^{-7} M **GG** in Dulbecco's Modified Medium in 50 mM TRIS buffer at pH 7.35 and with varying phosphate concentrations in the range from 10 to 400 mM.

Notably, not only was the response range of GG wider, its sensitivity was also slightly higher compared with **2-Me-4-OMe TG**. Indeed, the response range of **GG** extended to 400 mM, whereas **2-Me-4-OMe TG** was only effective at phosphate concentrations of up to 240 mM. In terms of sensitivity, the maximum change in the fluorescence decay time within the response range was ~ 0.4 ns versus the 0.25 ns change shown by **TG**. Even in the concentration range studied with **2-Me-4-OMe TG,** the decrease in the **GG** decay time was 15% higher.

*Fluorescence imaging microscopy of **GG** in preosteoblast cells*

The results obtained on glass slides suggest that this dye may have advantages over **2-Me-4-OMe TG** as an intracellular probe for phosphate using FLIM technology. First, we tested whether **GG** satisfies the additional requirements of water solubility and membrane permeability by performing experiments on live cells and obtaining images from the dye in the cell. Based on the fluorescence intensity upon excitation at 485 nm of the cells during dye loading, it was concluded that the dye accumulates efficiently inside the cytosol but is excluded from the cell nucleus. To gain more insight into the temporal behaviour of the **GG** fluorescence emission in the

Organic & Biomolecular Chemistry Accepted Manuscript

This journal is © The Royal Society of Chemistry 2012

intracellular medium and the effect of different concentrations of phosphate ions, we used MC3T3-E1 preosteoblast cells treated with α−toxin and various concentrations of pH 7.35 phosphate buffer. The MC3T3-E1 murine preosteoblast cell line is a well-established model for osteoblast differentiation. The ability of osteoblasts to transport extracellular phosphate into the cell through a transporter has been established.[5]
Treatment with α−toxin generated 1.5-nm membrane pores, which permitted the diffusion of low molecular weight compounds, including both **GG** and phosphate anions, without the loss of cytosolic proteins and high molecular weight compounds.[30] FLIM images were recorded and analysed using the procedure described in the Experimental section. Figure 8 shows the FLIM images revealing changes in the decay time of the dye inside the MC3T3-E1 osteoblast cells treated with α−toxin versus the spiked phosphate concentration ranging from 10 to 240 mM after applying an arbitrary colour scale. Although the range of decay times is narrow, the use of an appropriate colour scale permits a reasonably accurate estimate of the different phosphate concentrations inside the permeabilised cells.

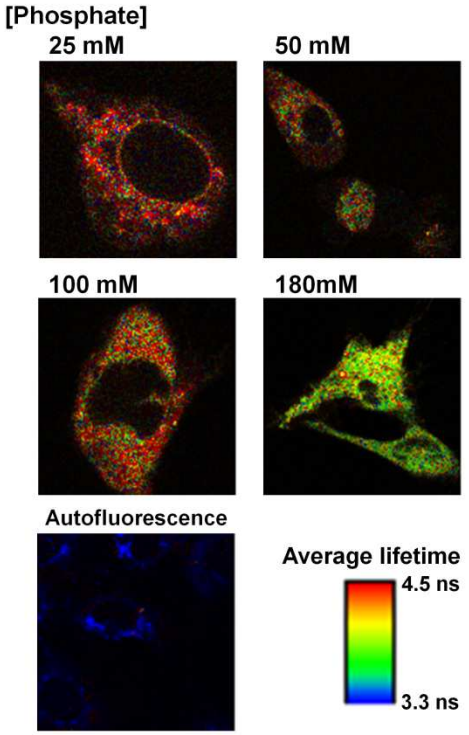

Figure 8. FLIM images of 1×10^{-7} **GG** dye in the cytoplasm of MC3T3-E1 osteoblast cells treated with α−toxin after incubation in extracellular media with different phosphate concentrations. The image labelled as autofluorescence corresponds to the FLIM image of the cells collected without the dye.

Conclusions

In summary, we designed and synthesised a new dye that has chemical reactivity and spectral characteristics similar to those of 2-Me-4-OMe TG but shows a higher pKa for the neutral and anion equilibrium. The new dye, referred to as **GG**, undergoes the same phosphate-mediated reaction in the excited state as does fluorescein and its derivatives, giving rise to fluorescence decay traces that are dependent on the phosphate concentration in the medium. The advantages of **GG** with respect to 2-Me-4-OMe TG, a previously tested intracellular phosphate sensor, are its ability to detect a wider range of phosphate concentrations along with an additional slight increase in sensitivity, measured as the ratio of the phosphate concentration/decay time. To prove the usefulness of **GG** as a phosphate sensor in the cellular cytoplasm, MC3T3-E1 preosteoblast cells permeabilised with α−toxin and submerged in PBS solutions at different phosphate concentrations at pH 7.35 were used. The FLIM images recovered show that **GG** adequately reflects the intracellular phosphate concentration.

Acknowledgements

This work was supported by grants CTQ2010-20507/BQU and CTQ-2011.22455 from the Ministerio Español de Ciencia e Innovación and P09-FQM-4571 from Regional Government of Andalucía. AO acknowledges the grant P10-FQM-6154 from the Conserjeria de Economia, Innovacion, Ciencia y Empleo (Junta de Andalucia). DM thanks Spanish MICINN (project CTQ-2011.22455) for her contract.

Notes and references

[a]Department of Organic Chemistry, Faculty of Sciences, University of Granada, C. U. Fuentenueva s/n, 18071 Granada, Spain.

[b]Department of Physical Chemistry, Faculty of Pharmacy, University of Granada, Cartuja Campus, 18071 Granada, Spain.

[c]Department of Inorganic Chemistry, University of Granada, C. U. Fuentenueva s/n, 18071 Granada, Spain.

E-mail: luiscrovetto@ugr.es; jmcuerva@ugr.es

Electronic Supplementary Information (ESI) available: [details of any supplementary information available should be included here]. See DOI: 10.1039/b000000x/

1. M. K. Kuimova, G. Yahioglu, J. A. Levitt and K. Suhling, *J. Am. Chem. Soc.*, 2008, 130, 6672-6673.
2. B. Hötzer, R. Ivanov, T. Brumbarova, P. Bauer and G. Jung, *FEBS J.*, 2012, 279, 410-419.
3. K. Okabe, N. Inada, C. Gota, Y. Harada, T. Funatsu and S. Uchiyama, *Nat. Commun.*, 2012, 3, 1714/1711-1714/1719,S1714/1711-S1714/1721.
4. M. Y. Berezin and S. Achilefu, *Chem. Rev. (Washington, DC, U. S.)*, 2010, 110, 2641-2684.
5. G. R. Beck, Jr., B. Zerler and E. Moran, *Proc. Natl. Acad. Sci. U. S. A.*, 2000, 97, 8352-8357.
6. T. Schenk, N. M. G. M. Appels, E. D. A. van, H. Irth, U. R. Tjaden and d. G. J. van, *Anal. Biochem.*, 2003, 316, 118-126.
7. J. Hirose, H. Fujiwara, T. Magarifuchi, Y. Iguti, H. Iwamoto, S. Kominami and K. Hiromi, *Biochim. Biophys. Acta*, 1996, 1296, 103-111.

Organic & Biomolecular Chemistry Accepted Manuscript

8. H. Imamura, K. P. Huynh Nhat, H. Togawa, K. Saito, R. Iino, Y. Kato-Yamada, T. Nagai and H. Noji, *Proceedings of the National Academy of Sciences*, 2009, 106, 15651-15656.
9. M. Ito, S. Haito, M. Furumoto, Y. Uehata, A. Sakurai, H. Segawa, S. Tatsumi, M. Kuwahata and K.-i. Miyamoto, *Am. J. Physiol.*, 2007, 292, C526-C534.
10. M. R. Ganjali, M. Hosseini, Z. Memari, F. Faridbod, P. Norouzi, H. Goldooz and A. Badiei, *Anal. Chim. Acta*, 2011, 708, 107-110.
11. J. M. Paredes, M. D. Giron, M. J. Ruedas-Rama, A. Orte, L. Crovetto, E. M. Talavera, R. Salto and J. M. Alvarez-Pez, *J. Phys. Chem. B*, 2013, 117, 8143-8149.
12. J. Yguerabide, E. Talavera, J. M. Alvarez and B. Quintero, *Photochem. Photobiol.*, 1994, 60, 435-441.
13. J. M. Alvarez-Pez, L. Ballesteros, E. Talavera and J. Yguerabide, *J. Phys. Chem. A*, 2001, 105, 6320-6332.
14. N. Boens, W. Qin, N. Basaric, A. Orte, E. M. Talavera and J. M. Alvarez-Pez, *J. Phys. Chem. A*, 2006, 110, 9334-9343.
15. J. Widengren, V. Kudryavtsev, M. Antonik, S. Berger, M. Gerken and C. A. M. Seidel, *Anal. Chem.*, 2006, 78, 2039-2050.
16. T. Miura, Y. Urano, K. Tanaka, T. Nagano, K. Ohkubo and S. Fukuzumi, *J. Am. Chem. Soc.*, 2003, 125, 8666-8671.
17. T. Ueno, Y. Urano, K. Setsukinai, H. Takakusa, H. Kojima, K. Kikuchi, K. Ohkubo, S. Fukuzumi and T. Nagano, *J. Am. Chem. Soc.*, 2004, 126, 14079-14085.
18. T. Mineno, T. Ueno, Y. Urano, H. Kojima and T. Nagano, *Org. Lett.*, 2006, 8, 5963-5966.
19. R. Zhou and T. Ha, *Methods Mol. Biol.*, 2012, 922, 85-100.
20. Y. Urano, M. Kamiya, K. Kanda, T. Ueno, K. Hirose and T. Nagano, *J. Am. Chem. Soc.*, 2005, 127, 4888-4894.
21. J. M. Paredes, L. Crovetto, R. Rios, A. Orte, J. M. Alvarez-Pez and E. M. Talavera, *Phys. Chem. Chem. Phys.*, 2009, 11, 5400-5407.
22. L. Crovetto, J. M. Paredes, R. Rios, E. M. Talavera and J. M. Alvarez-Pez, *J. Phys. Chem. A*, 2007, 111, 13311-13320.
23. J. M. Paredes, A. Garzon, L. Crovetto, A. Orte, S. G. Lopez and J. M. Alvarez-Pez, *Physical Chemistry Chemical Physics*, 2012, 14, 5795-5800.
24. C. R. Schroeder, B. M. Weidgans and I. Klimant, *Analyst*, 2005, 130, 907-916.
25. A. M. Paradiso, R. Y. Tsien and T. E. Machen, *Proc. Natl. Acad. Sci. U. S. A.*, 1984, 81, 7436-7440.
26. M. L. Graber, D. C. DiLillo, B. L. Friedman and E. Pastoriza-Munoz, *Anal. Biochem.*, 1986, 156, 202-212.
27. L. D. Lavis, T. J. Rutkoski and R. T. Raines, *Anal. Chem.*, 2007, 79, 6775-6782.
28. A. Martinez-Peragon, D. Miguel, R. Jurado, J. Justicia, J. M. Alvarez-Pez, J. M. Cuerva and L. Crovetto, *Chem. - Eur. J.*, 2014, 20, 447-455.
29. H. Sudo, H. A. Kodama, Y. Amagai, S. Yamamoto and S. Kasai, *J. Cell Biol.*, 1983, 96, 191-198.
30. M. D. Giron, C. M. Havel and J. A. Watson, *Proc. Natl. Acad. Sci. U. S. A.*, 1994, 91, 6398-6402.
31. J. R. Lakowicz, *Principles of Fluorescence Spectroscopy*, Springer, 3rd edn., 2006.
32. S. E. Braslavsky, A. U. Acuna, W. Adam, F. Amat, D. Armesto, T. D. Z. Atvars, A. Bard, E. Bill, L. O. Bjoern, C. Bohne, J. Bolton, R. Bonneau, H. Bouas-Laurent, A. M. Braun, R. Dale, K. Dill, D. Doepp, H. Duerr, M. A. Fox, T. Gandolfi, Z. R. Grabowski, A. Griesbeck, A. Kutateladze, M. Litter, J. Lorimer, J. Mattay, J. Michl, R. J. D. Miller, L. Moggi, S. Monti, S. Nonell, P. Ogilby, G. Olbrich, E. Oliveros, M. Olivucci, G. Orellana, V. Prokorenko, K. R. Naqvi, W. Rettig, A. Rizzi, R. A. Rossi, E. San Roman, F. Scandola, S. Schneider, E. W. Thulstrup, B. Valeur, J. Verhoeven, J. Warman, R. Weiss, J. Wirz and K. Zachariasse, *Pure Appl. Chem.*, 2007, 79, 293-465.
33. M. Maus, M. Cotlet, J. Hofkens, T. Gensch, S. F. C. De, J. Schaffer and C. A. Seidel, *Anal. Chem.*, 2001, 73, 2078-2086.
34. C. Hansch, A. Leo and R. W. Taft, *Chem. Rev.*, 1991, 91, 165-195.
35. K. S. Alongi and G. C. Shields, in *Annual Reports in Computational Chemistry*, ed. A. W. Ralph, Elsevier, 2010, vol. Volume 6, pp. 113-138.
36. K. C. Gross and P. G. Seybold, *Int. J. Quantum Chem.*, 2001, 85, 569-579.
37. Structures 3 and 4 showed the same trend (8.16 and 7.74 kJ mol-1 respectively). Nevertheless`, for compound 2 the calculated free energies for structures around the minimum of energy oscillated up to 3 kJ mol-1`, avoiding a reliable comparison with the other values.
38. In this case`, the torsion angle in the minimum energy structure is about 66°. When we artificially force the angle to 90 ° the situation is clearer and the proton transfer energy is only 1.04 kJ mol-1 with respect to 2-Me-4-OMe TG.
39. T. Nagano, *Proc. Jap. Acad., B*, 2010, 86, 837-847.
40. E. Cielen, A. Tahri, K. Ver Heyen, G. J. Hoornaert, F. C. De Schryver and N. Boens, *J. Chem. Soc., Perkin Trans. 2*, 1998, 1573-1580.
41. E. Cielen, A. Stobiecka, A. Tahri, G. J. Hoornaert, F. C. De Schryver, J. Gallay, M. Vincent and N. Boens, *J. Chem. Soc., Perkin Trans. 2*, 2002, 1197-1206.

Organic & Biomolecular Chemistry Accepted Manuscript

This journal is © The Royal Society of Chemistry 2012